Journal of Non-Crystalline Solids 356 (2010) 1867–1870

Contents lists available at ScienceDirect

Journal of Non-Crystalline Solids

journal homepage: www.elsevier.com/ locate/ jnoncrysol

Letter to the Editor

Zinc-based bulk metallic glasses

W. Jiao, K. Zhao, X.K. Xi, D.Q. Zhao, M.X. Pan, W.H. Wang *

Institute of Physics, Chinese Academy of Sciences, Beijing 100190, People's Republic of China

ARTICLE INFO

Article history:
Received 15 March 2010
Received in revised form 6 July 2010
Available online 7 August 2010

Keywords:
Metallic glass;
Zink-based glass

ABSTRACT

We report the fabrication and properties of zinc-based bulk metallic glasses (BMGs). The formation mechanism of the BMGs is also discussed. The combination properties of high corrosion resistance, low glass transition temperature T_g and high formability, low Young's modulus and density, low cost, harmless components to organisms and tunable degradation behavior make the Zn-based metallic glasses or metallic plastics (MPs) a potential candidate for micro- and nano-manufacturing materials and biomaterials.

Metallic glass has attracted substantial attention in the last two decades because of its scientific significance and potential engineering applications [1–5]. Much effort has been devoted to searching novel bulk metallic glasses (BMGs) especially for ordinary late transition metals (e.g. Fe, Co, Ni, Cu) based glassy alloys [6–13]. For engineering applications, low cost late transition metal-based bulk metallic glasses with high glass-forming ability are more applicable. Zinc, as the fourth most common metal in use, is widely used as an anti-corrosion agent and a good sacrificial anode in cathodic protection [14]. Zinc is also important for human beings' health, and it is the second most abundant transition metal element in organisms. Zinc as an ordinary late transition metal has been widely used as an addition element in alkaline earth such as Mg [15,16], Ca [17,18], and Sr [19] based BMGs, which have great potential to be used as biodegradable implants [16].

Recently, a series of metallic glasses with exceptionally low T_g (around 100 °C or 373 K), high glass-forming ability and thermal stability and large supercooled liquid region has been developed [4,5,18–21]. These BMGs [e.g. Ce-, CaLi-, La-, Sr-, and Au-based BMGs] exhibit the temperature driven transition from metallic-like to plastic-like behaviors, and are then also named as metallic plastics (MPs). The thermoplastic processing, shaping and forming at a temperature range near room temperature of these metallic plastics have a remarkable advantage to replicate very fine microstructures even in nanometer scale [4,5,18]. This is of importance for micro electro-mechanical systems and other areas where high precision parts are needed. Therefore, these MPs can be used as potential materials for micro- and nano-manufacturing [4,5]. However, the metallic plastics either show poor corrosion resistance because of the highly reactive nature of base elements (such as Ce-, Ca-, Mg-, and Sr-based MPs) or have high cost such as Au- and Pt-based MPs. The melting point of Zinc (692.68 K) is relatively low compared with Ca, Ce, La, Mg, and Yb [22]. Zinc also has high corrosion resistance and low cost [14]. Therefore, according to the found correlation between melting temperature and glass transition temperature T_g [23], the metallic glasses based on zinc could have low T_g, and low cost and high corrosion resistance which could be used as ideal candidate for micro- and nano-manufacturing and for biomaterials. On the other hand, the Zn-based MPs with unique properties could act as an appropriate system to study some fundamental issues such as relaxation, glass transition, and glass formation mechanism. However, the formation of Zn-based BMGs has not been reported so far.

In this paper, we report the fabrication and properties of Zn-based bulk glassy metallic plastics. The mechanism for the formation of the metallic glasses is discussed based on found correlations. The Zn-based MPs like other metallic plastics such as Ce-, La-, LaCe-, Sr-, CaLi- and Au-based MPs indeed have low glass transition temperature T_g, high glass-forming ability and formability and low Young's modulus. The Zn-based glasses have a much better corrosion resistance compared with that of Ce-, Ca-, La- and Sr-based MPs and low cost compared with that of Au-, Pt-, and Pd-based MPs.

The Zn–Mg–Ca–Yb alloys of nominal composition listed in Table 1 were fabricated by induction melting of Zn, Mg, Ca, and Yb (purity better than 99.99%, 99.9%, 99% and 99.95% respectively) in quartz crucible in a purified argon atmosphere. The alloy melts were injected into copper molds to get cylinder or plate shapes. The glassy ribbon was produced by the melt-spinning method. The phase of the as-cast alloy was identified by X-ray diffraction (XRD) using a MAC M03 diffractometer with Cu *Ka* radiation source. The scanning speed was ~3°/min. Differential scanning calorimetry (DSC) (measuring temperature range was from room temperature to 873 K) was performed under a purified argon atmosphere in a Mettler Toledo DSC822e with a heating rate of 20 K min^{-1}. The elastic constants (including the Young's modulus E, the shear modulus G, the bulk modus K and Poisson's ratio ν) of the glasses are derived from the acoustic data

* Corresponding author.
E-mail address: whw@aphy.iphy.ac.cn (W.H. Wang).

0022-3093/$ – see front matter © 2010 Elsevier B.V. All rights reserved.
doi:10.1016/j.jnoncrysol.2010.07.017

Table 1
The values of the T_g, T_x, supercooled liquid temperature region, ΔT, T_l, reduced glass transition temperature T_{rg} ($=T_g/T_l$), the parameter describing formability in supercooled liquid region, $S=\Delta T/(T_l-T_g)$ [5], ρ (with accuracy of ~5%) and compressive fracture strength σ of Zn-based MPs (with accuracy of ~5%). The data of Ca- [17], Mg- [24], and other glasses are listed for comparison.

Materials	T_g (K)	T_x (K)	ΔT (K)	T_l (K)	T_{rg}	S	ρ (g/cm^3)	σ (MPa)
$Zn_{40}Mg_{11}Ca_{31}Yb_{18}$	396 ± 1	421 ± 1	25 ± 1	667 ± 1	0.594	0.10	4.298	663
$Zn_{40}Mg_{11}Ca_{35}Yb_{14}$	393 ± 1	420 ± 1	27 ± 1	658 ± 1	0.597	0.10	–	–
$Ca_{65}Mg_{15}Zn_{20}$	375 ± 1	410 ± 1	35 ± 1	630 ± 1	0.595	0.14	2.050	340
$Ca_{65}Li_{9.96}Mg_{8.54}Zn_{16.5}$	317 ± 1	339 ± 1	22 ± 1	581 ± 1	0.546	0.23	1.956	530
$Yb_{62.5}Zn_{20}Mg_{17.5}$	367 ± 1	398 ± 1	31 ± 1	655 ± 1	0.561	0.11	6.516	–
$Ce_{70}Al_{10}Cu_{20}$	341 ± 1	408 ± 1	67 ± 1	722 ± 1	0.471	0.18	6.699	490
$Mg_{65}Cu_{25}Y_{10}$	428 ± 1	492 ± 1	64 ± 1	757 ± 1	0.55	0.19	3.284	680
$Au_{49}Ag_{5.5}Pd_{2.3}Cu_{26.9}Si_{16.3}$	403 ± 1	457 ± 1	54 ± 1	655 ± 1	0.615	0.21	12.2	900
$Pt_{57.5}Cu_{14.7}Ni_{5.3}P_{22.5}$	509 ± 1	598 ± 1	89 ± 1	813 ± 1	0.626	0.29	15.02	1470

and density. The density ρ was measured by Archimedes' principle in deionized water. The acoustic data was taken from MATEC 6600 ultrasonic system with a measuring sensitivity of 0.5 ns, and a carrying frequency of 10 MHz. The samples with a gauge aspect ratio of 2:1 were cut out of the as-cast 2 mm rods for uniaxial compression tests on an Instron 5500R1186 machine at a strain rate of 1×10^{-4} s^{-1}.

We developed the Zn-based MPs based on the Ca–Mg–Zn ternary alloy system [17]. When increasing the Zn content in the ternary alloy, we find that the glass-forming ability (GFA) markedly decreases with the increase of Zn content as shown in Fig. 1(a). Rare earth element addition can significantly improve the GFA in many metallic glass systems [24], we then added rare earth Yb into the Zn–Mg–Ca alloy and found that a suitable addition of Yb improves its GFA effectively. The XRD patterns in Fig. 1 indicate that the GFA is significantly enhanced by the suitable addition of ytterbium. The alloy can only be cast into ribbons for about 10 at.% Yb addition. As Yb content increases to 18 at.% in the Zn–Mg–Ca alloy, the crystalline phases of $CaZn_2$ and Mg_2Ca are suppressed and cylinder-shaped amorphous rods with diameters of up to 2 mm can be fabricated by conventional copper mold cast. While as the content of ytterbium increases up to 24 at.%, the sharp peak associated to crystalline appears again. This kind of phenomenon, which has also been observed in many glass-forming systems, is due to that the appropriate alloying Yb can suppress the Laves like crystalline phases such as $CaZn_2$ and Mg_2Ca as shown in Fig. 1(a) and enhance the GFA of the Zn–Mg–Ca–Yb system. The photograph of the as-cast $Zn_{40}Mg_{11}Ca_{31}Yb_{18}$ MP both in cylinder and plate shapes is shown in Fig. 1(b). The surfaces of the Zn-based MPs appear reflective and smooth like that of other MPs and other BMGs.

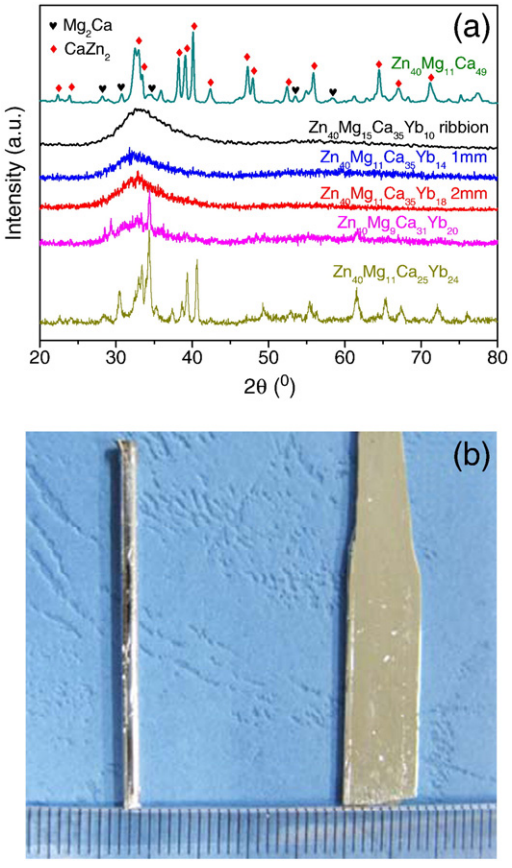

Fig. 1. (a) The XRD patterns of Zn–Mg–Ca–Yb alloys. (b) The photograph of the as-cast $Zn_{40}Mg_{11}Ca_{31}Yb_{18}$ alloys in cylinder and plate shapes.

The DSC traces of the Zn-based MPs are presented in Fig. 2 focusing on the glass transition and crystallization behaviors. The inset of the figure reveals the melting behavior of $Zn_{40}Mg_{11}Ca_{31}Yb_{18}$. The result further confirms the glassy nature of the as-cast alloy as it shows distinct glass transition and sharp crystallization peak. The exact values of T_g, crystallization temperature T_x, liquidus temperature T_l, and supercooled liquid region ΔT are listed in Table 1. The T_g of Zn-based MP (393–396 K) is slightly higher than that of Au-based MP [21], and the low T_g makes it possible to be plastically processed near ambient conditions such as processing in hot water or silicon oil. The parameter describing formability in supercooled liquid region, $S=\Delta T/(T_l-T_g)$ [Ref. 5] of the Zn-based MPs is about 0.10 (see Table 1), which is close to that of Ca-, Mg-, Yb-, and Ce-based MPs [17,18,20,25]. The density of the MP is about 4.3 g/cm [3], which can be classified into the light metallic glass family. The specific strength (σ/ρ) is about 154 MPa cm^3 g^{-1} and is higher than that of Au- and Pt-based MPs. For $Zn_{40}Mg_{11}Ca_{31}Yb_{18}$, its microhardness is about 1.8 GPa, and its Young's modulus is about 28.8 GPa which is comparable to that of a human bone (~10 to 30 GPa). The elastic strain is ~2%, and the fracture strength σ is 660 MPa. Fig. 3 shows the comparison of the

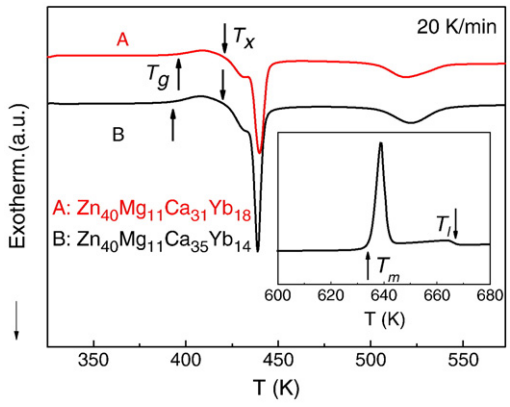

Fig. 2. The DSC curves of Zn–Mg–Ca–Yb alloys. The inset presents the melting behavior.

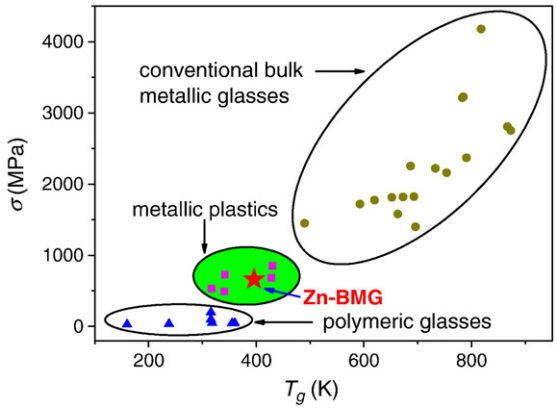

Fig. 3. Relation between T_g and fracture strength σ for metallic plastics based on Ce, La, Ca, Sr and Au, conventional bulk metallic glasses such as Zr-, Cu-, Fe-, and Ni-based glasses and some typical polymeric glasses including polypropylene(PP), polystyrene (PS), polymethylmethacrylate (PMMA), and nylon.

Zn-based MP to other known MPs and BMGs. The Zn-based MPs exhibit similar T_g values and mechanical properties as other metallic plastics. Compared to conventional bulk metallic glasses, the low T_g makes Zn-based MPs easily to be processed, evenly like polymeric plastics. However, the fracture strength of Zn-based MPs is nearly one order of magnitude higher than that of polymeric plastics.

Unlike the noble metal (e.g. Au-, Pt-based MPs) based MPs, the Ca-, Sr-, Mg-, and Ce-based MPs show poor corrosion resistance in water or humid condition because of the highly reactive behavior of their base elements. This reactive nature is a limiting factor for their practical applications. We investigated the corrosion behavior of the Zn-based MPs and compared it with that of $Ca_{65}Mg_{15}Zn_{20}$. Fig. 4 contrasts the degradation behavior of $Zn_{40}Mg_{11}Ca_{31}Yb_{18}$ and $Ca_{65}Mg_{15}Zn_{20}$ MPs. In the beginning, both MPs show shiny metallic surfaces (Fig. 4(a)). When immersed into distilled water, the surface of $Ca_{65}Mg_{15}Zn_{20}$ alloys was covered by bubbles coming from the corrosion reaction. While at the same time, the surface of $Zn_{40}Mg_{11}Ca_{31}Yb_{18}$ has no obvious change as shown in Fig. 4(b). Fig. 4(c) shows the state of both alloys immersed in distilled water for 90 min. The surface of $Zn_{40}Mg_{11}Ca_{31}Yb_{18}$ is still quite lustrous indicating quite stability in water. While for $Ca_{65}Mg_{15}Zn_{20}$, its surface became black and rough, and the obvious degradation process occurs accompanied without gassing. After 2 weeks of being immersed in distilled water, as shown in Fig. 4(d) the surface of $Zn_{40}Mg_{11}Ca_{31}Yb_{18}$ nearly has not been changed but $Ca_{65}Mg_{15}Zn_{20}$ has been almost fully degraded. The time dependence of the weight change percent (WCP) of Zn-based MP immersed in deionized water is given in Fig. 4(e). For more than one week, no remarkable weight change was observed in the Zn-based MP. In contrast, after being immersed in distilled water for two weeks, $Ca_{65}Mg_{15}Zn_{20}$ had fully degraded, only some spalled corrosion power product was left. We also investigate the oxidation behavior of Zn-based MPs using the similar method in Ref. [26]. For about one month, the surface of Zn-based MPs is still shiny indicating high oxidation resistance. We also note that, their degradation behavior can be tuned by changing the ratio of Zn and Ca, and the tunable degradation capability is important for biological applications [16].

The desirable properties combination of the Zn-based BMGs arises from the fortuitous value of T_g and high corrosion resistance which results from a Zn-based element with the lower melting temperature and high corrosion resistance among the metal elements. Sufficient data on melting temperature and T_g of various BMGs show that there is clear correlation [23,27]: the lower value of the melting temperature (T_m) of main components gives lower T_g. On the other hand, the T_m of BMGs shows a good correlation with a weighted average of the T_{mi} for the constituent elements as [27]: $T_m = \Sigma f_i \cdot T_{mi}$, where f_i denotes the atomic percentage of the constituent. The results imply that the

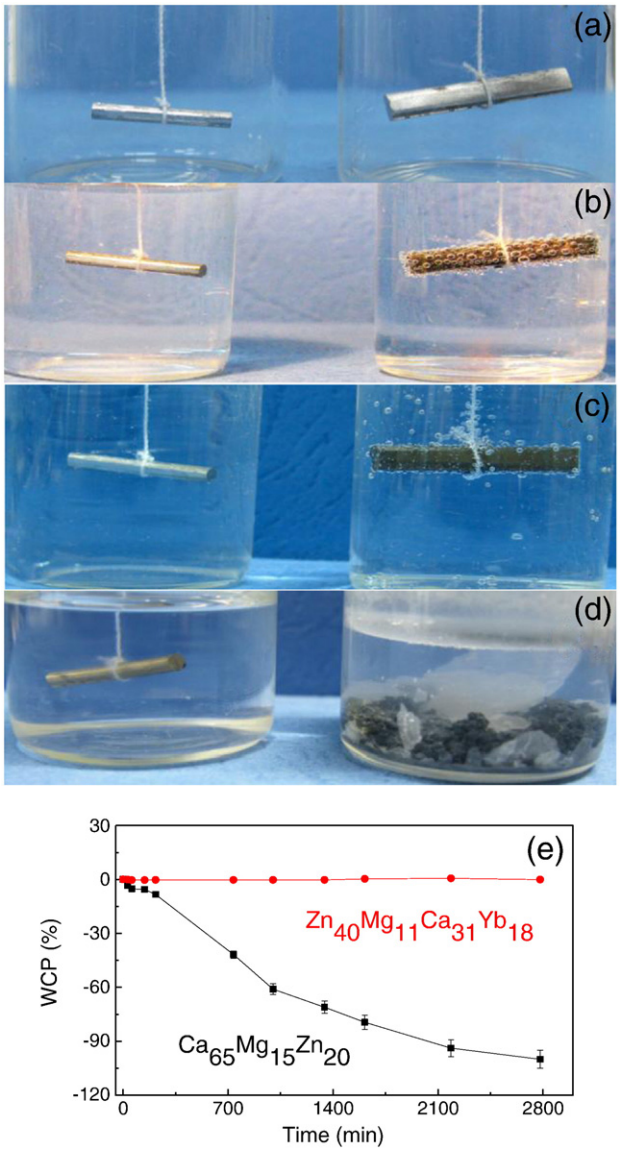

Fig. 4. Corrosion resistance behaviors of $Zn_{40}Mg_{11}Ca_{31}Yb_{18}$ and $Ca_{65}Mg_{15}Zn_{20}$ MPs. (a) Before distilled water was added. (b) As soon as distilled water was added. (c) Immersed in distilled water for 90 min. (d) Immersed in distilled water for two weeks. (e) The time dependence of the weight change percent of Zn-based MP immersed in deionized water.

value of T_g of a BMG depends strongly on the T_m of its components. In BMGs the base element usually determines their physical properties [23]. These established correlations provide useful guidelines for the development of the polymer-like BMGs by the selection of components with low T_m. This method is believed to be not limited to the Zn-based MPs but also has implications for other novel BMG explorations. In the fundamental research point of view, as one of the most stable metallic plastics, Zn-based MP is a model system to investigate structural relaxation and supercooled liquid state in alloys. For example, the glass can be used to study the long-term (weeks to months) ageing in metallic glasses by low temperature annealing. Such long-term ageing, which is not expected in other metallic glasses with high T_g, could assist in understanding some long-standing issues concerning slow relaxation kinetics in glasses.

In summary, the Zn-based BMGs are synthesized. The combination properties of the low cost, low T_g and high formability, and high corrosion resistance to oxidation and corrosion make the Zn-based MPs potential materials for micro- and nano-manufacturing. The harmless components to organisms, the tunable degradation rate

controlled by varying the relative ratio of constitutes, and low Young's modulus and density and high manufacturability make the Zn-based MPs promising candidates for biomedical uses.

Acknowledgements

Financial support is from the NSF of China (Numbers 50731008, 50921091 and 50890171) and MOST 973 of China (Numbers 2007CB613904 and 2010CB731600). Experimental aid and discussions of J.F. Li, J. Q. Wang, H. B. Ke, J. Yi, B. A. Sun and X. X. Xia are appreciated.

References

[1] W.L. Johnson, MRS Bull. 24 (1999) 42.
[2] A. Inoue, Acta Mater. 48 (2000) 279.
[3] A.L. Greer, Mater. Today 12 (2009) 14.
[4] W.H. Wang, Adv. Mater. 21 (2009) 4524.
[5] J. Schroers, Adv. Mater. doi:10.1002/adma.200902776.
[6] J. Shen, Q.J. Chen, J.F. Sun, H.B. Fan, G. Wang, Appl. Phys. Lett. 86 (2005) 151907.
[7] Z. Bian, M.X. Pan, Y. Zhang, W.H. Wang, Appl. Phys. Lett. 81 (2002) 4739.
[8] A. Inoue, B.L. Shen, H. Koshiba, H. Kato, A.R. Yavari, Nat. Mater. 2 (2003) 661.
[9] M.B. Tang, D.Q. Zhao, M.X. Pan, W.H. Wang, Chin. Phys. Lett. 21 (2004) 901.
[10] Y.X. Wang, H. Yang, G. Lim, Y. Li, Scr. Mater. 62 (2010) 682.
[11] H.X. Li, J.E. Gao, Z.B. Jiao, Y. Wu, Z.P. Lu, Appl. Phys. Lett. 95 (2009) 161905.
[12] D.H. Xu, G. Duan, W.L. Johnson, Phys. Rev. Lett. 92 (2004) 245504.
[13] K.F. Yao, C.Q. Zhang, Appl. Phys. Lett. 90 (2007) 061901.
[14] K.M. Hambidge, N.F. Krebs, J. Nutr. 137 (4) (2007) 1101.
[15] X. Gu, G.J. Shiflet, F.Q. Guo, S.J. Poon, J. Mater. Res. 20 (2005) 1935.
[16] B. Zberg, P.J. Uggowitzer, J.F. Loffler, Nat. Mater. 8 (2009) 887.
[17] O.N. Senkov, D.B. Miracle, V. Keppens, Metel. Mater. Trans. A 39 (2008) 1888.
[18] (a) J.F. Li, D.Q. Zhao, M.L. Zhang, W.H. Wang, Appl. Phys. Lett. 93 (2008) 171907; (b) S. Li, R.J. Wang, M.X. Pan, D.Q. Zhao, W.H. Wang, J. Non-cryst. Solids 354 (2008) 1080; (c) Y.X. Wei, B. Zhang, R.J. Wang, D.Q. Zhao, M.X. Pan, W.H. Wang, Script Mater. 54 (2006) 599.
[19] K. Zhao, J.F. Li, D.Q. Zhao, M.X. Pan, W.H. Wang, Scr. Mater. 61 (2009) 1091.
[20] B. Zhang, D.Q. Zhao, W.H. Wang, A.L. Greer, Phys. Rev. Lett. 94 (2005) 205502.
[21] W. Zhang, H. Guo, M.W. Chen, C.L. Qin, A. Inoue, Scr. Mater. 61 (2009) 744.
[22] http://www.webelements.com/zinc/physics.html.
[23] W.H. Wang, J. Appl. Phys. 99 (2006) 093506.
[24] W.H. Wang, Prog. Mater. Sci. 52 (2007) 540.
[25] J.Q. Wang, W.H. Wang, H.Y. Bai, Appl. Phys. Lett. 94 (2009) 041910.
[26] B.R. Barnard, P.K. Liaw, R.A. Buchanan, O.N. Senkov, D.B. Miracle, Mater. Trans. 48 (2007) 1870.
[27] Z. Li, J. Li, Appl. Phys. Lett. 94 (2009) 061913.